JPET Fast Forward. Published on March 15, 2017 as DOI: 10.1124/jpet.116.238022
This article has not been copyedited and formatted. The final version may differ from this version.

JPET #238022

Dual Inhibition of Bruton's Tyrosine Kinase and Phosphoinositide-3-Kinase p110δ as a Therapeutic Approach to Treat Non-Hodgkin's B cell Malignancies

Jennifer Alfaro[1], Felipe Pérez de Arce, Sebastián Belmar, Glenda Fuentealba, Patricio Avila, Gonzalo Ureta, Camila Flores, Claudia Acuña, Luz Delgado, Diana Gaete, Brahmam Pujala, Anup Barde, Anjan K. Nayak, TVR Upendra, Dhananjay Patel, Shailender Chauhan, Vijay K. Sharma, Stacy Kanno, Ramona G. Almirez, David T. Hung, Sarvajit Chakravarty, Roopa Rai, Sebastián Bernales, Kevin P. Quinn, Son M. Pham, Emma McCullagh[1]

Translational Research Group, Fundación Ciencia y Vida *(J.A., F.P., S.B., G.F., P.A., G.U., C.F., C.A., L.D., D.A.)*

Biological Sciences Department, Facultad de Ciencias Biológicas, Universidad Andrés Bello *(F.P., S.B.)*

Chemistry Group, Integral BioSciences, Pvt. Ltd. *(B.P., A.B., A.K.N, TVR.U., D.P, S.C., V.K.S.)*

Discovery Research, Medivation, Inc. now Pfizer *(S.K., R.G.A, D.T.H., S.C., R.R., S.B., K.P.Q., S.M.P., E.M.)*

JPET Fast Forward. Published on March 15, 2017 as DOI: 10.1124/jpet.116.238022
This article has not been copyedited and formatted. The final version may differ from this version.

JPET #238022

Running Title

Dual Inhibition of BTK and PI3Kδ to Treat B cell Cancers

Corresponding Author:

Emma McCullagh

525 Market St. 36th Fl

San Francisco, CA 94105

(415) 829-4109

Emmamccullagh@yahoo.com

Text pages: 24

Number of tables: 4

Number of Figures: 6 + 2 supplementary figures

Number of References: 32

Number of words in abstract: (max 250) 238

Number of words in introduction: (max 750 word) 747

Number of words in discussion: (max 1500 words) 1285

Nonstandard abbreviations:

AKT	protein kinase B
$AUC_{0-\infty}$	area under the plasma concentration-time curve from time 0 to infinity
AUC_{last}	area under the plasma concentration-time curve up to the last nonzero concentration
BCR	B cell receptor
BMX/Etk	epithelial and endothelial tyrosine kinase
BTK	Bruton´s tyrosine kinase
CL	systemic clearance
CLL	chronic lymphocytic leukemia
C_{max}	maximum concentration in plasma
DAG	diacylglycerol
ERK 1/2	extracellular signal-regulated kinase 1/2
F	absolute oral bioavailability
FBS	fetal bovine serum
FDA	Food and Drug Administration
FRET	fluorescence resonance energy transfer
HTRF	homogeneous time resolved fluorescence
IgD	immunoglobulin D
IgM	immunoglobulin M
IP3	inositol-1,4,5-triphosphate
ITAM	immunoreceptor tyrosine-based activation motif
ITK	IL-2 inducible T-cell kinase dimethyl sulfoxide

JPET Fast Forward. Published on March 15, 2017 as DOI: 10.1124/jpet.116.238022
This article has not been copyedited and formatted. The final version may differ from this version.

LC-MS/MS	liquid chromatography with tandem mass spectrometry
Lyn	Lck/Yes novel tyrosine kinase
MCL	mantel cell lymphoma
NHL	non-Hodgkin's lymphoma
PBS	phosphate buffered saline
PCR	polymerase chain reaction
PI3K	phosphatidylinositol-3-kinase
PI3Kδ	phosphatidylinositol-3-kinase delta
PIP_2	phosphatidylinositol-4,5-bisphosphate
PK	pharmacokinetic
PKC	protein kinase C
PLC-γ2	phospholipase C-γ2
RT	room temperature
Syk	spleen tyrosine kinase
$t_{1/2}$	elimination half-life
TEC	Tec protein tyrosine kinase
t_{max}	time of maximum concentration in plasma
V_d	volume of distribution

Recommended Section: Drug Discovery and Translational Medicine

JPET Fast Forward. Published on March 15, 2017 as DOI: 10.1124/jpet.116.238022
This article has not been copyedited and formatted. The final version may differ from this version.

Abstract

Although new targeted therapies such as ibrutinib and idelalisib have made a large impact on non-Hodgkin's lymphoma (NHL) patients, the disease is often fatal because patients are initially resistant to these targeted therapies or because they eventually develop resistance. New drugs and treatments are necessary for these patients. One attractive approach is to inhibit multiple parallel pathways that drive the growth of these hematologic tumors and possibly prolonging the duration of the response and reducing resistance. Early clinical trials have tested this approach by dosing two drugs in combination in NHL patients. We have discovered a single molecule **MDVN1003** that inhibits Bruton's tyrosine kinase (BTK) and phosphatidylinositol-3-kinase delta (PI3Kδ), two proteins regulated by the B cell receptor (BCR) that drive the growth of many NHLs. In this report, we show that this dual inhibitor prevents the activation of B cells and inhibits the phosphorylation of protein kinase B (AKT) and extracellular signal-regulated kinase 1/2 (ERK 1/2), two downstream mediators that are important for this process. Additionally, **MDVN1003** induces cell death in a B cell lymphoma cell line but not in an irrelevant erythroblast cell line. Importantly, we found that this orally bioavailable dual inhibitor reduced tumor growth in a B cell lymphoma xenograft model more effectively than either ibrutinib or idelalisib. Taken together these results suggest that dual inhibition of these two key pathways by a single molecule could be a viable approach for treatment of NHL patients.

JPET Fast Forward. Published on March 15, 2017 as DOI: 10.1124/jpet.116.238022
This article has not been copyedited and formatted. The final version may differ from this version.

Introduction

Non-Hodgkin's lymphomas (NHLs) are among the most common of human cancers and despite advancements of medical treatments and improvements in patient outcomes, the disease has a 30% mortality rate within the first five years after diagnosis (Howlader N, 2014; Swerdlow et al., 2016). Activation of BCR signaling is a significant mechanistic driver of the development and growth of B cell derived lymphoid tumors (Buchner and Muschen, 2014; Burger, 2016). Basal BCR signaling is necessary for the survival of B cells (Verkoczy et al., 2007; Wang et al., 2013) and signaling through the complex pathway is amplified during B cell activation (Woyach et al., 2012). The BCR is comprised of a membrane immunoglobulin complex, the ligation of which results in the phosphorylation of the cytoplasmic ITAMs (immunoreceptor tyrosine-based activation motif) of BCR co-receptors by two kinases, Lyn (Lck/Yes novel tyrosine kinase) and Syk (spleen tyrosine kinase). Propagation of the signal occurs via several parallel and interconnected pathways. Two important kinases downstream of the BCR are BTK and PI3Kδ (Seda and Mraz, 2015).

BTK is a member of the Tec family of tyrosine kinases and is recruited to the cell membrane after the activation of the BCR. Together with Syk, BTK phosphorylates phospholipase C-γ2 (PLC-γ2) producing the classic second messengers diacylglycerol (DAG) and inositol-1,4,5-triphosphate (IP_3) from phosphatidylinositol-4,5-bisphosphate (PIP_2). DAG activates protein kinase C (PKC) and IP_3 triggers the release of intracellular calcium, resulting in the activation of several downstream signaling molecules including ERK 1/2 (Tomlinson et al., 2001). PI3Kδ is also recruited to the cell membrane and activated in

response to BCR signaling. PI3K is a heterodimer comprised of the p85 regulatory subunit and the p110 catalytic subunit, which in B cells is the δ isoform. PI3Kδ is involved in recruiting BTK to the cell membrane and phosphorylates and activates several downstream signaling molecules including AKT (Fruman and Rommel, 2014). The BTK and PI3Kδ signaling pathways are not insulated from one another and there is evidence of crosstalk between them (Puri et al., 2013). Both BTK and PI3Kδ are involved in normal B cell signal propagation but have been identified as being aberrantly activated in many B cell malignancies (Seda and Mraz, 2015). These proteins are the targets of the approved therapies, ibrutinib (Pan et al., 2007), an irreversible BTK inhibitor, and idelalisib (Lannutti et al., 2011), a reversible PI3Kδ inhibitor.

Ibrutinib blocks the enzymatic activity of BTK through covalent binding to a conserved cysteine residue (Cys 481) in the active site (Honigberg et al., 2010). Ibrutinib was approved by the FDA for use in mantel cell lymphoma (MCL), chronic lymphocytic leukemia (CCL) and Waldenström's macroglobulinemia patients. Idelalisib is a highly selective ATP competitive inhibitor of PI3Kδ (Lannutti et al., 2011; Marini et al., 2016) and has been approved for use in CLL, follicular cell NHL and relapsed small lymphocytic lymphoma patients (Do et al., 2016).

While the approval of these targeted therapies by the FDA was a significant advance, it has been reported that about 30% of MCL and CLL patients show primary resistance to ibrutinib (Tucker and Rule, 2015). Furthermore, a subset of patients that initially respond and receive prolonged treatment of ibrutinib eventually relapse due to the development of mutations in BTK that prevent the covalent binding of ibrutinib or

JPET Fast Forward. Published on March 15, 2017 as DOI: 10.1124/jpet.116.238022
This article has not been copyedited and formatted. The final version may differ from this version.

activating mutations in PLC-γ2 (Byrd et al., 2013; Wang et al., 2013; Smith, 2015). The resistance to idelalisib is not as well understood. Several reports have suggested that combination dosing of ibrutinib and idelalisib could be advantageous since targeting parallel pathways downstream of the BCR could reduce the risk of signal switching leading to escape from tumor growth inhibition (Jones and Byrd, 2014; Mathews Griner et al., 2014; Zhang et al., 2014; de Rooij et al., 2015; Burger, 2016).

In this report, we describe proof-of-concept preclinical studies with tool compound **MDVN1003**, a first-in-class dual inhibitor of BTK and PI3Kδ kinases (Pujala et al., 2016). We found that **MDVN1003** inhibits B cell activation upon BCR cross-linking *ex vivo* and *in vivo*, a phenomenon dependent on BTK and PI3Kδ. Additionally, **MDVN1003** induces apoptosis and decreases viability of DOHH-2 cells, an NHL cell line. Finally, **MDVN1003**, an orally bioavailable molecule in mouse, rat and dog, showed significant anti-tumor effects in an NHL xenograft model in mice. This effect was similar to that seen with combination dosing of ibrutinib and idelalisib in the same model and greater than each of these drugs dosed as single agents. Our results suggest that a dual inhibitor of BTK and PI3Kδ could be an effective treatment strategy for B cell lymphoma patients.

Materials and Methods

Reagents and tumor cell lines

Ibrutinib (CAS 936563-96-1) and idelalisib (CAS 870281-82-6) were purchased from ChemShuttle (Union City, CA). Compounds **MDVN1003**, **MDVN1001** and **MDVN1002** were synthesized at Integral BioSciences, Pvt. Ltd., Noida, India. All tumor cell lines were

JPET Fast Forward. Published on March 15, 2017 as DOI: 10.1124/jpet.116.238022
This article has not been copyedited and formatted. The final version may differ from this version.

purchased from the American Type Culture Collection and were tested for mycoplasma by PCR. All revived cells were used within 20 passages, and cultured for less than 6 months. Ramos and DOHH2 cells were maintained in RPMI-1640 medium containing 10% heat-inactivated FBS supplemented with penicillin and streptomycin.

Enzymatic Kinase Assays

In vitro kinase activity assays were performed by Reaction Biology Corporation (www.reactionbiology.com) as described on their website and as described previously (Pujala et al., 2016).

Assessment of BCR dependent signaling levels

Ramos cells were pretreated for 30 minutes with compounds (0.1 µM or 1 µM final concentration) and then stimulated with α-human IgM (1.3 µg/ml) (#109-006-129, Jackson Laboratories) for 5 minutes. Levels of pAKT (Cell Signaling #5473), AKT (Cell Signaling #9272), pErk (T202, Y204) (Cell Signaling #4377) and ERK (Cell Signaling #4396) were detected by western blot using ChemiDoc Imaging System (Biorad).

Measuring B cells activation by CD69 expression

Splenocytes (1 x 10^6 cells/well) were seeded in a 24 well plate and pretreated for 30 min with compounds at indicated concentrations and then activated for 4 h with α-mouse IgD (3 µg/ml) (Accurate Chemical, YULLOMD6-05). Cells were stained with α-B220 PE (BD Pharmingen #553090), α-CD69 APC (Miltenyi Biotech #130-103-947) and with live/dead

fixable aqua dead cell kit (Life Technologies #L34957) and analyzed by flow cytometry using a MACSQuant Analyzer 10 flow cytometer. At each concentration of compound tested, the inhibition of B cell activation was calculated as the percentage of live B cells expressing CD69 in the presence of the compound divided by the percentage of live B cells expressing CD69 in the vehicle control. Splenocytes from three individual mice were treated independently per condition tested. The IC_{50} was calculated from the average of the three independent experiments and curve fitting was done by non-linear regression using GraphPad Prism.

Viability assay

DOHH-2 or HEL 92.1.7 cells were seeded in a 96 well white plates overnight at a density of 5000 cells/well. Cells were treated with compounds at the indicated concentrations for 72 h. Cell viability was measured using Cell Titer-glo kit (Promega) as described by the manufacturer. The IC_{50} was calculated from the curve fitted to the data points by non-linear regression using GraphPad Prism.

Apoptosis Assay

DOHH-2 cells were seeded in a 24 well plate at 0.5 x 10^6 cells/well. Cells were then treated with compounds at 1 µM for 4 h and apoptosis was measured by flow cytometry (MACSquant 10 Analyzer) using Annexin V FITC apoptosis detection kit (BD Pharmingen #556547).

Pharmacokinetic Analysis

All animal studies were done as per approved protocols by the Institutional Animal Care and Use Committee at Medivation or its subsidiaries. See supplementary information for experimental details of mouse, rat and dog PK studies.

Measuring B cell activation by CD69 expression *in vivo*

BALB/c mice were orally dosed with compounds (n=3 per group) at indicated concentration for 30 min and then mice were injected intravenously in the tail vein with 100 μg of α-IgD (Accurate Chemical, YULLOMD6-05) for 5 h. Splenocytes were isolated and stained and analyzed as described above. The percentage of live B cells that express CD69 from mice treated with α-IgD and compound was normalized to the percentage of live B cells that express CD69 from mice treated with α-IgD alone.

Mouse xenograft model

All animal studies were done as per approved protocols by the Institutional Animal Care and Use Committee at Medivation or its subsidiaries.

DOHH-2 cells were maintained in RPMI1640 medium supplemented with 10% FBS and were passaged twice weekly. While in exponential growth phase, 5 x 10^6 DOHH2 cells in 0.1 ml PBS (1:1 ratio with matrigel) were inoculated into the right flanks of 6-7 week old female CB17/SCID mice (denoted as day 0). When the average tumor volume reached 118 mm^3, mice were randomly grouped into 8 groups (n = 10 per group). Tumor volume and body weight was measured twice a week. The experiment was terminated when the

JPET Fast Forward. Published on March 15, 2017 as DOI: 10.1124/jpet.116.238022
This article has not been copyedited and formatted. The final version may differ from this version.

average tumor volume of the vehicle group reached > 2000 mm^3 and plasma and tumor samples were collected from each mouse (n=3 mice per group were sacrificed 5 min before the final dose, n=3 mice per group were sacrificed 30 min post final dose and n=4 mice per group were sacrificed 6 h post final dose). Statistical analysis (Kruskal-Wallis corrected for multiple comparisons) was done on the tumor volumes of the groups over time.

Results

As described (Pujala et al., 2016), we aimed to discover reversible dual BTK and PI3Kδ inhibitors based on the similarities between a reversible BTK inhibitor PCI-29732 (Pan et al., 2007; Marcotte et al., 2010) and a PI3Kδ/γ dual inhibitor, SW13 (Berndt et al., 2010). We identified three compounds (Figure 1), two of which are more potent against one of the two receptors and one compound that is a more potent dual inhibitor (Table 1 and synthesis in Supplementary Information). On the one hand, **MDVN1001** is a potent BTK inhibitor (IC_{50} 0.9 nM) and a relatively weak PI3Kδ inhibitor (IC_{50} 149 nM). On the other hand, **MDVN1002** strongly inhibited PI3Kδ (IC_{50} 25.9 nM) more than it did BTK (IC_{50} 695 nM). However, the dual inhibitor, **MDVN1003**, potently inhibited both kinases; BTK with an IC_{50} of 32.3 nM and PI3Kδ with an IC_{50} of 16.9 nM. As expected, the control compounds, idelalisib and ibrutinib, inhibited one kinase more strongly than the other. Idelalisib, an ATP competitive, reversible inhibitor of PI3Kδ, inhibited PI3Kδ with an IC_{50} of 1.2 nM, while it did not measurably inhibit BTK at any concentration tested. Ibrutinib, an

JPET Fast Forward. Published on March 15, 2017 as DOI: 10.1124/jpet.116.238022
This article has not been copyedited and formatted. The final version may differ from this version.

irreversible inhibitor of BTK, potently inhibited BTK (IC_{50} 0.142 nM), and weakly inhibited PI3Kδ (IC_{50} 640 nM).

To investigate the effects of these molecules on signaling through the BCR pathway, phosphorylation of ERK 1/2 and AKT was measured in the Ramos Burkitt's B cell lymphoma cell line. Ramos cells were pre-treated with vehicle or 0.1 μM of idelalisib, ibrutinib, **MDVN1001**, **MDVN1002**, **MDVN1003** or an equimolar co-treatment of idelalisib and ibrutinib (subsequently referred to as "combo"). Cells were treated with α-human IgM for 5 min to crosslink and activate the BCR. Levels of phosphorylated ERK 1/2 and AKT were detected by western blot (Figure 2). Treatment with α-human IgM increased the levels of phosphorylated AKT and ERK 1/2 as compared to the vehicle alone, indicating the BCR signaling pathway was activated (Figure 2, lanes 1 and 2). Ibrutinib and idelalisib treatments significantly reduced the levels of pERK 1/2 and pAKT. Neither **MDVN1001** nor **MDVN1002** significantly affected levels of pAKT or pERK 1/2 when tested at 0.1 μM. However, these compounds did inhibit the phosphorylation of AKT and ERK1/2 at higher concentrations (Supplementary Figure 1). Combination treatment of idelalisib and ibrutinib potently inhibited levels of both pAKT and pERK 1/2 (Figure 2). The combination treatment **MDVN1001** and **MDVN1002** (combo MDVN) also inhibited the phosphorylation of AKT and ERK1/2, however not as potently as the combination treatment of the two approved inhibitors (Figure 2, Supplementary Figure 1). Treatment with the dual BTK/PI3Kδ inhibitor compound, **MDVN1003,** inhibited the phosphorylation of AKT and pERK 1/2 at both the low concentration (0.1 μM) and the high concentration (1 μM) and did so more potently than the combination of the **MDVN1001** and **MDVN1002** (Figure 2,

Supplementary Figure 1). Taken together, these data show that **MDVN1003** is a more potent inhibitor of BCR signaling than either **MDVN1001** or **MDVN1002** dosed individually or in combination and suggest that the dual inhibition of BTK and PI3Kδ may have a synergistic effect on downstream signaling molecules.

We wanted to further investigate the potential synergy of inhibiting both BTK and PI3Kδ in B cell lymphomas using ibrutinib, idelalisib and **MDVN1003** as tool compounds. These compounds provided us the necessary tools to study treatment with monotherapies and dual inhibition. **MDVN1003** is more potent than either **MDVN1001** or **MDVN1003** (or the combination of both) in the cell-based assay and allowed us to study dual inhibition in a single molecule.

To understand the selectivity profile of **MDVN1003** and how it compares to those of ibrutinib and idelalisib, we tested these compounds in a kinase panel at 1 µM. Idelalisib is a highly selective PI3Kδ inhibitor and inhibited four other kinases (out of 374 tested) greater than 50%. Ibrutinib inhibited 34 kinases (out of 374 tested) more than 50% (Figure 3). **MDVN1003** behaved similarly to ibrutinib in the kinase panel and inhibited 50 kinases (out of 402 tested) at greater than 50%, with a preference for tyrosine kinases (Figure 3). Among the kinases most potently inhibited by **MDVN1003** were the BTK, PI3Kδ and the related Tec- and PI3K-family kinases (Figure 3, Table 2).

We next investigated the effects of **MDVN1003** on the activation of primary B cells *ex vivo*. Mouse splenocytes were pre-treated with ibrutinib, idelalisib, combo or **MDVN1003** for 30 min. Cells were treated with anti-human IgD for 4 h to activate B cells. Anti-IgD crosslinks the surface immunoglobulin and activates B cell, which upregulates the

JPET Fast Forward. Published on March 15, 2017 as DOI: 10.1124/jpet.116.238022
This article has not been copyedited and formatted. The final version may differ from this version.

early B cell activation marker CD69 (Sancho et al., 2005). Activated B cells were detected by flow cytometry as B22+CD69+ in a gate of live cells. The inhibition of B cell activation was measured by the percentage of live B cells that expressed CD69 on the cell surface in treated samples as compared to the α-IgD control. Ibrutinib and idelalisib potently inhibited B cell activation, with IC_{50}s of 6.9 nM and 5.4 nM, respectively (Figure 4A, Table 3). Idelalisib, but not ibrutinib, produced full inhibition of B cell activation. The combo treatment of both compounds showed a modest additive effect with an IC_{50} of 1.1 nM (Figure 4A, Table 3) and also produced full inhibition of B cell activation. **MDVN1003** inhibited B cell activation with an IC_{50} of 25.2 nM (Figure 4A, Table 3). While less potent, **MDVN1003** was equally efficacious to idelalisib and the combo treatment and fully inhibited B cell activation.

Signaling through the BCR is often a driver of tumor growth in B cell malignancies (Buchner and Muschen, 2014) and it has been reported that both ibrutinib and idelalisib reduce cell viability and induce apoptosis in NHL B cell lines (Honigberg et al., 2007; Lannutti et al., 2011; Qu et al., 2015). To determine whether **MDVN1003** behaved similarly to the approved drugs, we measured the effect of **MDVN1003** on the viability of DOHH-2 cells, a non-Hodgkin's B cell lymphoma line that expresses BTK and PI3Kδ. After 72 h of treatment. **MDVN1003** effectively killed DOHH-2 cells with an IC_{50} of 1.34 µM, while the IC_{50}s for ibrutinib and idelalisib were 0.023 µM and 0.86 µM, respectively (Figure 4B, Table 3). The IC_{50} for the combo treatment was 0.0084 µM, suggesting an additive effect on cell viability of inhibiting both BTK and PI3Kδ. The cytotoxicity induced by these compounds was determined to be apoptosis as indicated by the significant population of

Annexin V+ propidium iodide (PI)- cells in treatment groups as compared to the vehicle control ($P < 0.0001$, one-way ANOVA) (Figure 4C). Combination treatment of **MDVN1001**, the BTK inhibitor, and **MDVN1002**, the PI3Kδ inhibitor, also showed an additive effect on cell viability of DOHH-2 cells with an IC50 of 0.87 µM, as compared to IC50s of 1.47 µM with **MDVN1001** alone and 2.75 µM with **MDVN1002** alone (Supplementary Figure 2). Although a modest effect, these data suggest a benefit of dual inhibition of BTK and PI3Kδ.

To understand if the cytotoxicity of these compounds was dependent on inhibition of BTK and PI3Kδ, we tested the effects of the compounds on viability of HEL 92.1.7 erythroblast-like cells that do not express these kinases. The IC_{50}s of ibrutinib, idelalisib, the combo and **MDVN1003** were all greater than 10 µM (Table 3), suggesting that these compounds are preferentially cytotoxic in cells that express BTK and PI3Kδ.

In order to study the pharmacology of **MDVN1003** *in vivo*, we investigated the pharmacokinetic (PK) properties of this molecule across species. The PK profiles of **MDVN1003** in mice, rats, and dogs, after a single oral dose are shown in Figure 5. The noncompartmental analysis PK parameters of **MDVN1003** in mice, rats, and dogs are summarized in Table 4. Following oral administration in mice, **MDVN1003** showed rapid absorption with a t_{max} of 0.25 h and then declined with a biexponential decay and a $t_{1/2}$ of 1.3 h (Figure 5, Table 4). The absolute oral bioavailability (F) was acceptable at 40%. Following intravenous administration in mice, **MDVN1003** showed low systemic clearance (0.6 L/h/kg) that was 13% of hepatic blood flow in the mouse [Q_H = 4.7 L/h/kg, (Davies and Morris, 1993)] and moderate volume of distribution [V_d = 3.4 L/kg] as shown in Table 4. Following oral administration in rats, **MDVN1003** showed rapid absorption with a t_{max} of

0.25 h and then declined with a biexponential decay with a $t_{1/2}$ of 1.2 h (Figure 5). The absolute oral bioavailability (F) was an acceptable 31%. Following intravenous administration in rats, **MDVN1003** showed high systemic clearance (4.94 L/h/kg) that was 150% of hepatic blood flow in the rat [Q_H = 3.31 L/h/kg, (Davies and Morris, 1993)] and moderate volume of distribution [V_d = 2.0 L/kg] as shown in Table 4. Following oral administration in dog, **MDVN1003** showed rapid absorption with a t_{max} of 0.42 h and then declined with a biexponential decay with a $t_{1/2}$ of 1.5 h (Figure 5). The absolute oral bioavailability (F) was a moderately high 62%. Following intravenous administration in dog, **MDVN1003** showed moderate systemic clearance (1.23 L/h/kg) that was 66% of hepatic blood flow in the dog [Q_H = 1.85 L/h/kg, (Davies and Morris, 1993)] and moderate volume of distribution [V_d = 1.0 L/kg] as shown in Table 4.

Given the low clearance and acceptable oral bioavailability of **MDVN1003** in mice, we aimed to show pharmacological efficacy, as proof of concept, in two *in vivo* mouse models; a model of B cell activation and a xenograft model of non-Hodgkin's B cell lymphoma. To test the effect of the compounds on B cell activation *in vivo*, BALB/c mice were prophylactically dosed with different oral doses of compound for 30 min prior to being challenged with an α-IgD antibody administered intravenously via the tail vein to activate BCR signaling for up to 5 h (Figure 6A). After the treatment, splenocytes were isolated and activated B cells were detected by flow cytometry as B220+CD69+ in a gate of live cells. With no α-IgD treatment, between 3 to 5% of B cells were active basally (CD69+) in spleens (data not shown). In mice treated orally with vehicle and intravenously with α-IgD, around 30% of B cells were CD69+ (data not shown). This value was set to 100%

activation and the percentages of CD69+ B cells in the drug treated mice were normalized to the percentage of CD69+ B cells in the α-IgD treated control group. Ibrutinib effectively inhibited (>50%) B cell activation at all doses tested (10, 50 and 100 mg/kg) while idelalisib only inhibited B cell activation by 50% at 10 mg/kg (Figure 6B) but was effective at higher doses. **MDVN1003** did not inhibit B cell activation at 10 mg/kg but inhibited activation by 75% at 50 and 100 mg/kg (Figure 6B). The lack of a dose response at 50 and 100 mpk of **MDVN1003** may suggest that absorption of this compound is already saturated at 50 mpk.

Given that **MDVN1003** induced cell death in DOHH-2 cells and inhibited B cell activation *in vivo*, we tested whether this compound was able to inhibit tumor growth *in vivo* in a DOHH-2 B cell lymphoma xenograft model. Six to seven week old CB17/SCID mice were inoculated in the right flank with 5 x 10^6 DOHH-2 cells. Mice were grouped (n = 10/group) and dosing began when tumors reached an average of 100 mm^3. Dosing was terminated when the average tumor volume of the vehicle group reached 2000 mm^3. Mice were placed into one of eight groups and dosed with vehicle, two doses of ibrutinib (15 or 30 mg/kg), two doses of idelalisib (25 or 50 mg/kg), two combinations of ibrutinib and idelalisib (15 mg/kg ibrutinib/25 mg/kg idelalisib or 30 mg/kg ibrutinib/50 mg/kg idelalisib) or one dose level of **MDVN1003** (100 mg/kg). Ibrutinib was dosed once daily due to its irreversible binding and idelalisib and **MDVN1003** were both dosed twice daily. Mice were monitored for body weight and tumor volume over the 21 days of dosing. The body weight of the mice was unaffected by the treatments (Figure 6C). Tumor growth was slowed by combination treatment of ibrutinib and idelalisib and by treatment with **MDVN1003** (Figure 6D, E). On the final day of dosing (day 31 post inoculation), ibrutinib at

JPET Fast Forward. Published on March 15, 2017 as DOI: 10.1124/jpet.116.238022
This article has not been copyedited and formatted. The final version may differ from this version.

either 15 mg/kg or 30 mg/kg reduced average tumor volume by 15.7% and 24.7%, respectively, and idelalisib at 25 mg/kg or 50 mg/kg reduced average tumor volume by 6.6% and 14.2%, respectively, as compared to the vehicle control group (not statistically significant). When dosed in combination, the average tumor volume of the ibrutinib (15 mg/kg) and idelalisib (25 mg/kg) low combo group was reduced by 38.1% as compared to the vehicle group, while tumors in the ibrutinib (30 mg/kg) and idelalisib (50 mg/kg) high combo group were reduced by 57.9% on average as compared to the vehicle control group ($P < 0.001$, Kruskal-Wallis corrected for multiple comparisons). Treatment with **MDVN1003** reduced tumor growth by 45.2% ($P < 0.01$, Kruskal-Wallis corrected for multiple comparisons).

Discussion

The potential advantage of dual inhibition of BTK and PI3Kδ for treatment of NHL lies in the possibility of treating refractory patients or overcoming developed resistance to either BTK or PI3Kδ single inhibitors due to the synergistic or additive effects of blocking two BCR pathway targets. Co-dosing BTK and PI3Kδ single inhibitors is one approach to gain the advantage of dual inhibition. Pre-clinical evidence supports the notion that inhibiting these two pathways could result in synergistic or additive effects. Combination treatments of JeKo1 cells, a MCL cell line, with ibrutinib and idelalisib resulted in decreased adhesion to fibronectin, a BCR dependent process, as compared to cells treated with each drug individually (de Rooij et al., 2015). The authors found a strong synergistic effect with the dual treatment. In another example, combination treatment of BCWM.1

Waldenström's macroglobulinemia cells with both ibrutinib and TG Therapeutics' highly selective second generation PI3Kδ inhibitor, TGR-1202, resulted in increased cell death as compared to treatment with the individual drugs (Davids et al., 2016).

In this report, we corroborate the findings that co-treatment of B cells with ibrutinib and idelalisib results in superior effects to those seen with either drug dosed individually. The phosphorylation of downstream signaling molecules AKT and ERK 1/2 was significantly dampened in cells treated with both drugs as compared to each drug individually (Figure 2). Similarly in the xenograft model, co-dosing the two inhibitors more effectively reduced the tumor burden than dosing each compound separately (Figure 6). These data support the hypothesis that targeting two BCR-controlled pathways could be more efficacious than treatment with a monotherapy.

Preclinical data suggesting the potential synergism of inhibiting both BTK and PI3Kδ have spurred clinical trials of combination treatments. TG Therapeutics has several ongoing clinical studies with TGR-1202 (Vakkalanka et al., 2012) and ibrutinib for B cell malignancies including relapsed or refractory CLL and mantle MCL. TG Therapeutics has reported interim results from their phase I/Ib study of overall response rate of 82% in CLL and 60% in MCL but has yet to show a reduction in the rate of resistance (Davids et al., 2016).

While combination treatment of two separate BTK and PI3Kδ inhibitors does provide the advantage of being able to independently control the dose of each inhibitor, we tested the hypothesis that a dual inhibitor in a single molecule could be a potential therapeutic approach for NHL. Having the dual inhibition activity built into a single

molecule could ease the toxicology profile since there would be a single set of off target effects. The cost of treatment for patients may also be lower with a single molecule due to lower manufacturing and formulation costs (Shanafelt et al., 2015). We have described elsewhere our discovery of dual BTK and PI3Kδ inhibitors (Pujala et al., 2016) and here we report that one of these dual inhibitors does exhibit properties similar to combination dosing of ibrutinib and idelalisib, albeit not as potent or selective.

MDVN1003, while a dual inhibitor of BTK and PI3Kδ, is not as potent an inhibitor as idelalisib and ibrutinib are against their primary targets as measured in *in vitro* enzymatic assays (Table 1). Despite the difference in potencies, **MDVN1003** inhibits the *in vitro* phosphorylation of AKT and ERK 1/2 as well as either ibrutinib or idelalisib. **MDVN1001** and **MDVN1002** are potent single inhibitors of BTK and PI3Kδ, respectively, but these compounds only inhibited the phosphorylation of AKT or ERK 1/2 at the higher concentration of 1 μM. This could be due to the lower potency of **MDVN1002** against PI3Kδ molecules or possibly to a difference in the cell permeability of **MDVN1001** and **MDVN1002**. Similarly to the combo treatment of ibrutinib and idelalisib, combination treatment with **MDVN1001** and **MDVN1002** showed an additive effect on the inhibition of the phosphorylation of AKT and ERK1/2 upon BCR activation and on cell viability of DOHH-2 cells. Taken together, the data suggest a synergistic effect of dual inhibition of BTK and PI3Kδ and by **MDVN1003**. This is further supported by the superior efficacy of **MDVN1003** in the xenograft model as compared to either ibrutinib or idelalisib dosed individually. The difference in potency of **MDVN1003** against BTK and PI3Kδ could explain why treatment with this compound is not as effective as combo dosing of ibrutinib and idelalisib *in vitro*

or *in vivo* (Figure 4 and 6). Further SAR would be required to identify more potent dual BTK and PI3Kδ inhibitors with good oral bioavailability that could be tested for better efficacy *in vivo*.

Another possibility for the superior performance of **MDVN1003** compared to monotherapy in the tumor xenograft model is that the antitumor effect could be unrelated to the inhibition of BTK or PI3Kδ. **MDVN1003** inhibits many kinases at 1 μM (Figure 3) so it is possible that the antitumor effect is not due to synergy of dual inhibition but instead due to the inhibition of another kinase that is required for the growth of DOHH-2 cells. The treatment of **MDVN1001**, **MDV1002** or the combo treatment of these molecules were similarly potent as **MDVN1003** in the cell viability assay raises the possibility that the effect on cell viability by these three molecules may not be completely driven by the inhibition of BTK and PI3Kδ. However, **MDVN1003** is not generally cytotoxic. This molecule, along with ibrutinib and idelalisib, did not induce cell death in HEL 92.1.7 erythroblasts (Table 3). These cells do not express BTK or PI3Kδ and any other kinase inhibited by **MDVN1003** was not sufficient to induce cytotoxicity. Further optimization of the tool compound **MDVN1003** is necessary to improve the selectivity profile and fully rule out off target effects.

In practice, ibrutinib is extremely effective and the 24-month progression free survival in the phase I and phase II studies of ibrutinib in CLL were greater than 80% (Tucker and Rule, 2015). However, 30% of patients are initially refractory to ibrutinib (Tucker and Rule, 2015) and even more become resistant after long term dosing (Byrd et al., 2013; Wang et al., 2013; Smith, 2015) so reducing the rate of resistance or increasing

the duration of response could be important for treating patients with B cell malignancies. A potential advantage of combination therapy of BTK and PI3Kδ inhibitors may be to reduce the rate of acquired resistance to either BTK or PI3Kδ inhibition and potentially be efficacious in patients initially resistant to treatment of either a BTK or a PI3Kδ inhibitor. However, the preclinical data reported here and elsewhere (Jones and Byrd, 2014; Mathews Griner et al., 2014; Zhang et al., 2014; de Rooij et al., 2015; Burger, 2016) do not directly test whether dual inhibition or co-dosing is efficacious in the case of resistance. To date, no preclinical or clinical studies have looked at the effects of co-treating with BTK and PI3Kδ inhibitors on the rates of resistance. In fact, there is a dearth of reagents with which to investigate these questions and a lack of knowledge around adaptive resistance to PI3Kδ inhibition.

In summary, our results show that dual inhibition of BTK and PI3Kδ by treatment with a single dual inhibitor could potentially improve the outcomes of NHL patients and may prevent resistance or extend the duration of response. While **MDVN1003** proved useful as an initial tool compound, further medicinal chemistry efforts are required to improve potency to achieve cytotoxic and tumor inhibitory effects that match the combination treatment with ibrutinib and idelalisib. Additional investigation is required to better understand the mechanisms by which resistance to ibrutinib and idelalisib occurs and generate reagents to better elucidate preclinical efficacy. The results presented here provide a proof of concept that a dual inhibitor of BTK and PI3Kδ in a single molecule can be developed and could be used as a viable approach for the treatment of B cell malignancies.

Acknowledgements

We thank Katherine Stack from Fundación Ciencia y Vida for help with animal studies; Ashu Gupta and the bioanalytical group at Integral BioSciences for the execution of key *in vitro* metabolism studies that produced important steps forward in the program. We acknowledge the skilled researchers at Reaction Biology and Crown Biosciences for their work.

Authorship Contributions

Participated in experimental design: McCullagh, Alfaro, Bernales, Quinn, Hung

Conducted experiments: Alfaro, Pérez de Arce, Avila, Gaete, Fuentealba, Kanno, Almirez, Flores, Belmar, Ureta, Delgado, Acuña

Contributed new reagents of analytic tools: Pham, Pujala, Barde, Nayak, Upendra, Patel, Chauhan, Sharma, Rai, Chakravarty

Performed data analysis: McCullagh, Alfaro, Quinn, Perez de Arce, Gaete, Fuentealba, Flores, Belmar, Ureta

Wrote or contributed to the writing of the manuscript: McCullagh, Alfaro, Pham, Rai, Quinn

References

Berndt A, Miller S, Williams O, Le DD, Houseman BT, Pacold JI, Gorrec F, Hon W-C, Liu Y, Rommel C, Gaillard P, Ruckle T, Schwarz MK, Shokat KM, Shaw JP and Williams RL (2010) The p110 δ crystal structure uncovers mechanisms for selectivity and potency of novel PI3K inhibitors. *Nature chemical biology* **6**:117-124.

Buchner M and Muschen M (2014) Targeting the B-cell receptor signaling pathway in B lymphoid malignancies. *Curr Opin Hematol* **21**:341-349.

Burger JA (2016) B-cell receptor signaling in chronic lymphocytic leukemia and other B-cell malignancies. *Clin Adv Hematol Oncol* **14**:55-65.

Byrd JC, Furman RR, Coutre SE, Flinn IW, Burger JA, Blum KA, Grant B, Sharman JP, Coleman M, Wierda WG, Jones JA, Zhao W, Heerema NA, Johnson AJ, Sukbuntherng J, Chang BY, Clow F, Hedrick E, Buggy JJ, James DF and O'Brien S (2013) Targeting BTK with ibrutinib in relapsed chronic lymphocytic leukemia. *N Engl J Med* **369**:32-42.

Davids MS, Kim HT, Nicotra A, Saveli A, Francoeur K, Hellman JM, Miskin H, Sportelli P, Rado T, Bashey A, Stampleman L, Rueter J, Boruchov A, Arnason JE, Jacobson CA, Fisher DC and Brown JR (2016) Preliminary Results of a Phase I/Ib Study of Ibrutinib in Combination with TGR-1202 in Patients with Relapsed/Refractory CLL or MCL, in *2016 Annual Congress of the European Hematology Association*, Copenhagen, Denmark.

Davies B and Morris T (1993) Physiological parameters in laboratory animals and humans. *Pharm Res* **10**:1093-1095.

de Rooij MF, Kuil A, Kater AP, Kersten MJ, Pals ST and Spaargaren M (2015) Ibrutinib and idelalisib synergistically target BCR-controlled adhesion in MCL and CLL: a rationale for combination therapy. *Blood* **125**:2306-2309.

Do B, Mace M and Rexwinkle A (2016) Idelalisib for treatment of B-cell malignancies. *Am J Health Syst Pharm* **73**:547-555.

Fruman DA and Rommel C (2014) PI3K and cancer: lessons, challenges and opportunities. *Nat Rev Drug Discov* **13**:140-156.

Honigberg LA, Smith AM, Chen J, Thiemann P and Verner E (2007) Targeting Btk in Lymphoma: PCI-32765 Inhibits Tumor Growth in Mouse Lymphoma Models and a Fluorescent Analog of PCI-32765 Is an Active-Site Probe That Enables Assessment of Btk Inhibition *In Vivo*. *Blood* **110**:1592-1592.

Honigberg LA, Smith AM, Sirisawad M, Verner E, Loury D, Chang B, Li S, Pan Z, Thamm DH, Miller RA and Buggy JJ (2010) The Bruton tyrosine kinase inhibitor PCI-32765 blocks B-cell activation and is efficacious in models of autoimmune disease and B-cell malignancy. *Proc Natl Acad Sci U S A* **107**:13075-13080.

Howlader N NA, Krapcho M, Garshell J, Miller D, Altekruse SF, Kosary CL, Yu M, Ruhl J, Tatalovich Z,Mariotto A, Lewis DR, Chen HS, Feuer EJ, Cronin KA (eds) (2014) SEER Cancer Statistics Review, 1975-2011, in, National Cancer Institute. Bethesda, MD, http://seer.cancer.gov/csr/1975_2011/.

Jones JA and Byrd JC (2014) How will B-cell-receptor-targeted therapies change future CLL therapy? *Blood* **123**:1455-1460.

Lannutti BJ, Meadows SA, Herman SE, Kashishian A, Steiner B, Johnson AJ, Byrd JC, Tyner JW, Loriaux MM, Deininger M, Druker BJ, Puri KD, Ulrich RG and Giese NA (2011) CAL-101, a p110delta selective phosphatidylinositol-3-kinase inhibitor for the treatment of B-cell malignancies, inhibits PI3K signaling and cellular viability. *Blood* **117**:591-594.

Marcotte DJ, Liu YT, Arduini RM, Hession CA, Miatkowski K, Wildes CP, Cullen PF, Hong V, Hopkins BT, Mertsching E, Jenkins TJ, Romanowski MJ, Baker DP and Silvian LF (2010) Structures of human Bruton's tyrosine kinase in active and inactive conformations suggest a mechanism of activation for TEC family kinases. *Protein Sci* **19**:429-439.

Marini BL, Samanas L and Perissinotti AJ (2016) Expanding the armamentarium for chronic lymphocytic leukemia: A review of novel agents in the management of chronic lymphocytic leukemia. *J Oncol Pharm Pract*.

Mathews Griner LA, Guha R, Shinn P, Young RM, Keller JM, Liu D, Goldlust IS, Yasgar A, McKnight C, Boxer MB, Duveau DY, Jiang JK, Michael S, Mierzwa T, Huang W, Walsh MJ, Mott BT, Patel P, Leister W, Maloney DJ, Leclair CA, Rai G, Jadhav A, Peyser BD, Austin CP, Martin SE, Simeonov A, Ferrer M, Staudt LM and Thomas CJ (2014) High-throughput combinatorial screening identifies drugs that cooperate with ibrutinib to kill activated B-cell-like diffuse large B-cell lymphoma cells. *Proc Natl Acad Sci U S A* **111**:2349-2354.

Pan Z, Scheerens H, Li SJ, Schultz BE, Sprengeler PA, Burrill LC, Mendonca RV, Sweeney MD, Scott KC, Grothaus PG, Jeffery DA, Spoerke JM, Honigberg LA, Young PR, Dalrymple SA and Palmer JT (2007) Discovery of selective irreversible inhibitors for Bruton's tyrosine kinase. *ChemMedChem* **2**:58-61.

Pujala B, Agarwal AK, Middya S, Banerjee M, Surya A, Nayak AK, Gupta A, Khare S, Guguloth R, Randive NA, Shinde BU, Thakur A, Patel DI, Raja M, Green MJ, Alfaro J, Avila P, Pérez de Arce F, Almirez RG, Kanno S, Bernales S, Hung DT, Chakravarty S, McCullagh E, Quinn KP, Rai R and Pham SM (2016) Discovery of Pyrazolopyrimidine Derivatives as Novel Dual Inhibitors of BTK and PI3K δ . *ACS Medicinal Chemistry Letters*.

Puri KD, Di Paolo JA and Gold MR (2013) B-cell receptor signaling inhibitors for treatment of autoimmune inflammatory diseases and B-cell malignancies. *Int Rev Immunol* **32**:397-427.

Qu F-L, Xia B, Li S-X, Tian C, Yang H-L, Li Q, Wang Y-F, Yu Y and Zhang Y-Z (2015) Synergistic suppression of the PI3K inhibitor CAL-101 with bortezomib on mantle cell lymphoma growth. *Cancer Biology & Medicine* **12**:401-408.

Sancho D, Gomez M and Sanchez-Madrid F (2005) CD69 is an immunoregulatory molecule induced following activation. *Trends Immunol* **26**:136-140.

Seda V and Mraz M (2015) B-cell receptor signalling and its crosstalk with other pathways in normal and malignant cells. *European Journal of Haematology* **94**:193-205.

Shanafelt T, Borah B, Finnes H, Chaffee K, Ding W, Leis J, Chanan-Khan A, Parikh S, Slager S, Kay N and Call T (2015) Impact of ibrutinib and idelalisib on the pharmaceutical cost of treating chronic lymphocytic leukemia at the individual and societal levels. *J Oncol Pract* **11**:252-258.

Smith MR (2015) Ibrutinib in B lymphoid malignancies. *Expert Opin Pharmacother* **16**:1879-1887.

Swerdlow SH, Campo E, Pileri SA, Harris NL, Stein H, Siebert R, Advani R, Ghielmini M, Salles GA, Zelenetz AD and Jaffe ES (2016) The 2016 revision of the World Health Organization classification of lymphoid neoplasms. *Blood* **127**:2375-2390.

Tomlinson MG, Woods DB, McMahon M, Wahl MI, Witte ON, Kurosaki T, Bolen JB and Johnston JA (2001) A conditional form of Bruton's tyrosine kinase is sufficient to activate multiple downstream signaling pathways via PLC Gamma 2 in B cells. *BMC Immunology* **2**:1-12.

Tucker DL and Rule SA (2015) A critical appraisal of ibrutinib in the treatment of mantle cell lymphoma and chronic lymphocytic leukemia. *Therapeutics and Clinical Risk Management* **11**:979-990.

Vakkalanka S, Viswanadha S, Boise LH, Sportelli P, Miskin H, Lonial S (2012) TGR-1202: A Novel, Targeted PI3Kδ Inhibitor in Multiple Myeloma. *Blood* **120**(21) 5018.

Verkoczy L, Duong B, Skog P, Ait-Azzouzene D, Puri K, Vela JL and Nemazee D (2007) Basal B cell receptor-directed phosphatidylinositol 3-kinase signaling turns off RAGs and promotes B cell-positive selection. *J Immunol* **178**:6332-6341.

Wang ML, Rule S, Martin P, Goy A, Auer R, Kahl BS, Jurczak W, Advani RH, Romaguera JE, Williams ME, Barrientos JC, Chmielowska E, Radford J, Stilgenbauer S, Dreyling M, Jedrzejczak WW, Johnson P, Spurgeon SE, Li L, Zhang L, Newberry K, Ou Z, Cheng N, Fang B, McGreivy J, Clow F, Buggy JJ, Chang BY, Beaupre DM, Kunkel LA and Blum KA (2013) Targeting BTK with ibrutinib in relapsed or refractory mantle-cell lymphoma. *N Engl J Med* **369**:507-516.

Woyach JA, Johnson AJ and Byrd JC (2012) The B-cell receptor signaling pathway as a therapeutic target in CLL. *Blood* **120**:1175-1184.

Zhang Q, Xia B, Qu F, Yuan T, Guo S, Zhao W, Li Q, Yang H, Wang Y and Zhang Y (2014) [Effect of PI3Kdelta inhibitor CAL-101 on myeloma cell lines and preliminary study of synergistic effects with other new drugs]. *Zhonghua Xue Ye Xue Za Zhi* **35**:926-930.

Footnotes

Financial support for this research was provided by Medivation, Inc., now Pfizer. Some authors are employees of Medivation, now Pfizer. Some authors are inventors on patents related to the subject matter.

[1]JA and EM contributed equally to this work.

Figure Legends

Figure 1: Novel structures afford BTK and PI3Kδ inhibitory activity to be dialed in and out. The structures of idelalisib, ibrutinib, and three novel compounds, **MDVN1001**, **MDVN1002** and **MDVN1003** are detailed. **MDVN1001**, **MDVN1002** and **MDVN1003** are enantiomerically pure but the absolute configuration has yet to be determined (asterisks in the structures mark the stereogenic centers).

Figure 2: BTK and PI3Kδ inhibitor compounds differentially inhibit the phosphorylation of downstream signaling molecules ATK and ERK. Ramos cell were pretreated with 0.1 μM of the indicated compounds or DMSO (vehicle and -) for 30 min. All samples except for the vehicle control were treated with α-IgM (1.3 μg/ml) for 5 min to activate BCR signaling. Levels of pAKT and pERK 1/2 and the corresponding total proteins were determined by western blot. Combo is equimolar (0.1 μM) treatment of ibrutinib and idelalisib.

Figure 3: The kinase profile of **MDVN1003** is similar to that of ibrutinib. Ibrutinib, idelalisib and **MDVN1003** were tested at 1 μM against > 350 kinases in enzymatic assays. The percentage of inhibition is plotted for each kinase. The values for ibrutinib are shown in blue in the top graph. The values for idelalisib are shown in red in the middle panel and the values for **MDVN1003** are shown in purple in the bottom panel. The kinases are organized by family as indicated above the graphs. The PI3Kδ family of kinases are highlighted by the orange line and the BTK family are highlighted by the green line.

Figure 4: **MDVN1003** inhibits B cell activation in mouse splenocytes and induces apoptosis in DOHH-2 B cell lymphoma cells. **A**. Splenocytes were pretreated with the indicated compounds at different concentration for 30 min and then treated with α-IgD (3 μg/ml) for 4 h to activate BCR signaling. Activated B cells were identified by flow cytometry as the B220+ CD69+ cells in a live gate. To calculate the effect of each compound on the inhibition of B cell activation, the percentage of B220+ CD69+ cells in each condition was normalized to the α-IgD vehicle control. The IC_{50} was calculated from the curve fitted to the data points by non-linear regression using GraphPad Prism. **B**. DOHH-2 cells were treated with compounds at the indicated concentrations for 72 h. Cell viability was measured as described in the Materials and Methods. The IC_{50} was calculated from the curve fitted to the data points by non-linear regression using GraphPad Prism. **C**. DOHH-2 cells were treated with compounds at 1 μM for 4 h and apoptosis was measured by flow cytometry using Annexin V FITC apoptosis detection kit. Apoptotic cells were determined as Annexin V+ PI- by flow cytometry. Dot plots from a representative experiment are shown above and a summary of the percentages of apoptotic cells from four independent experiments are plotted below (mean ± standard deviation, **** $P < 0.0001$, one-way ANOVA)

Figure 5: **MDVN1003** concentration-time profile following an oral dose in mouse, rat and dog. Mice, rats and dogs were treated orally (PO) or intravenously (data not plotted) and drug concentrations in plasma were monitored over time by LC-MS/MS analysis. The PK parameters are shown in Table 4.

Figure 6: **MDVN1003** inhibits B cell activation *in vivo* and inhibits tumor growth in a B cell lymphoma xenograft model. **A**. Scheme of the treatment conditions for experiment in **B**. **B**. BALB/c mice were orally dosed with compounds or vehicle (Veh and -) at indicated concentrations for 30 min. Mice in all groups except the vehicle control (Veh) were then dosed intravenously with α-IgD for 5 h. Splenocytes were isolated and stained with a live/dead marker, αB220 and αCD69 antibodies. Activated B cells were determined as B220+ CD69+ in a live gate by flow cytometry. Percentage of activated B cells post compound treatment was normalized to the percentage active B cells in the α-IgD control (- in graph). **C-E** Compounds were tested in a mouse xenograft model of NHL. Ibrutinib was dosed at 15 mg/kg (light blue) or 30 mg/kg (dark blue); idelalisib was dosed at 25 mg/kg (pink) or 50 mg/kg (red); combo low dosing group was 15 mg/kg ibrutinib and 25 mg/kg idelalisib (ibrutinib/idelalisib low, light green); combo high dosing group was 30 mg/kg ibrutinib and 50 mg/kg idelalisib (ibrutinib/idelalisib high, dark green); **MDVN1003** was dosed at 100 mg/kg. Ibrutinib was dosed orally once daily and the other two compounds were dosed orally twice daily. **C**. Average body weight of mice in each dosing group (mean ± standard deviation of n = 10 mice per group). **D**. Average tumor volume of mice in each dosing group (mean ± standard deviation, *** $P < 0.001$, Kruskal-Wallis). **E**. The tumor volume of each mouse in the dosing groups on the final day of dosing (day 31 post inoculation). The black line shown is the average tumor volume of each group and the colored lines are the standard deviations. (*** $P < 0.001$, ** $P < 0.01$, Kruskal-Wallis corrected for multiple comparisons).

JPET Fast Forward. Published on March 15, 2017 as DOI: 10.1124/jpet.116.238022
This article has not been copyedited and formatted. The final version may differ from this version.

Table 1: IC_{50} values for compounds against PI3Kδ and BTK in kinase inhibition assay

IC_{50} (nM)	PI3Kδ	BTK
idelalisib	1.2	>100000
ibrutinib	640	0.142
MDVN1001	149	0.9
MDVN1002	25.9	695
MDVN1003	16.9	32.3

JPET Fast Forward. Published on March 15, 2017 as DOI: 10.1124/jpet.116.238022
This article has not been copyedited and formatted. The final version may differ from this version.

Table 2: IC_{50} values for compounds against BTK and PI3Kδ kinase family members

IC_{50} (nM)	idelalisib	ibrutinib	**MDVN1003**
PI3Kα	354	>100000	275
PI3Kβ	90.2	>100000	708
PI3Kγ	30	>1000	107
BMX/ETK	>100000	<0.1	44.5
ITK	>100000	19.3	>300
TEC	>100000	<0.1	211

JPET Fast Forward. Published on March 15, 2017 as DOI: 10.1124/jpet.116.238022
This article has not been copyedited and formatted. The final version may differ from this version.

Table 3: IC_{50} values for the inhibition of B cell activation in primary mouse splenocytes and cytotoxic effects in DOHH-2 lymphoma and HEL 92.1.7 cells

IC_{50} (nM)	**Primary B cell activation (CD69)**	**DOHH-2 cell viability**	**HEL 92.1.7 cell viability**
ibrutinib	6.9	23	>10,000
idelalisib	5.4	860	>10,000
combo	1.1	8.4	>10,000
MDVN1003	25.2	1340	>10,000

JPET Fast Forward. Published on March 15, 2017 as DOI: 10.1124/jpet.116.238022
This article has not been copyedited and formatted. The final version may differ from this version.

Table 4: Pharmacokinetic parameters of MDVN1003 across species

	Species	**Mouse**	**Rat**	**Dog**
	Dose	**2 mg/kg**	**2 mg/kg**	**1 mg/kg**
Intravenous	C_{max} (µM)	5.57 ± 1.66	3.53 ± 0.037	3.34 ± 0.244
	AUC_{last} (µM*h)	7.63 ± 0.59	0.968 ± 0.0122	2.04 ± 0.571
	Terminal $t_{1/2}$ (h)	7.16 (N=2)	0.285 ± 0.149	0.62 ± 0.27
	CL (L/h/kg)	0.594 ± NA	4.94 ± 0.065	1.23 ± 0.327
	V_d (L/kg)	3.445 ± NA	2.02 ± 1.044	1.02 ± 0.153
	Dose	**10 mg/kg**	**5 mg/kg**	**3 mg/kg**
Oral	C_{max} (µM)	11.3 ± 1.29	1.27 ± 0.686	3.32 ± 1.42
	t_{max} (h)	0.25	0.25	0.417 ± 0.144
	AUC_{last} (µM*h)	15.2 ± 1.87	0.751 ± 0.274	3.77 ± 1.66
	Terminal $t_{1/2}$ (h)	1.26	1.17 ± 0.464	1.48 ± 1.26
	Bioavailability (%)	39.8 ± 4.71	31 ± 11.3	61.7 ± 32.1

JPET Fast Forward. Published on March 15, 2017 as DOI: 10.1124/jpet.116.238022
This article has not been copyedited and formatted. The final version may differ from this version.

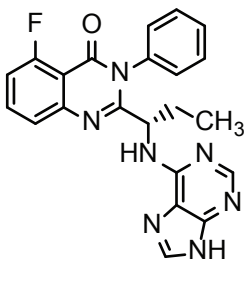

idelalisib

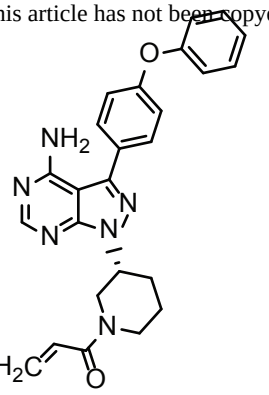

ibrutinib

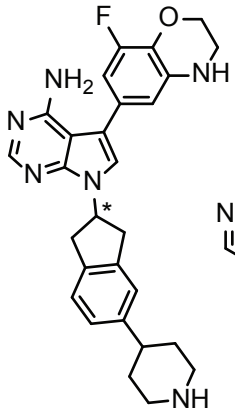

MDVN1001

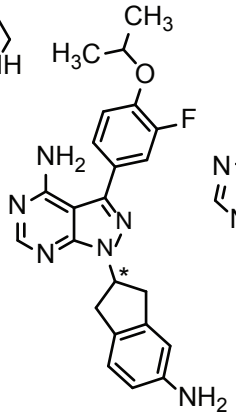

MDVN1002

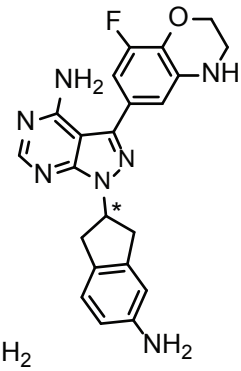

MDVN1003

JPET Fast Forward. Published on March 15, 2017 as DOI: 10.1124/jpet.116.238022
This article has not been copyedited and formatted. The final version may differ from this version.

Figure 2

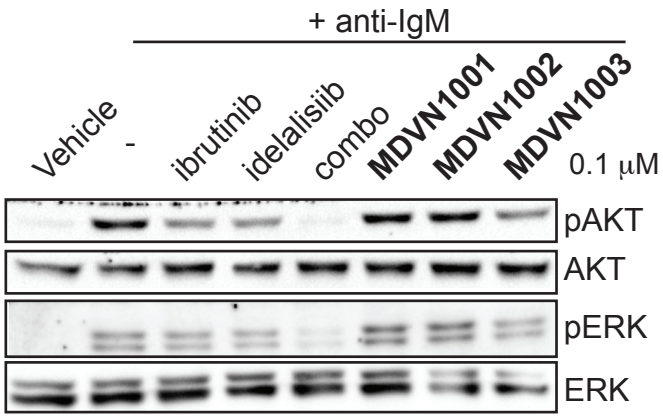

JPET Fast Forward. Published on March 15, 2017 as DOI: 10.1124/jpet.116.238022
This article has not been copyedited and formatted. The final version may differ from this version.

Figure 3

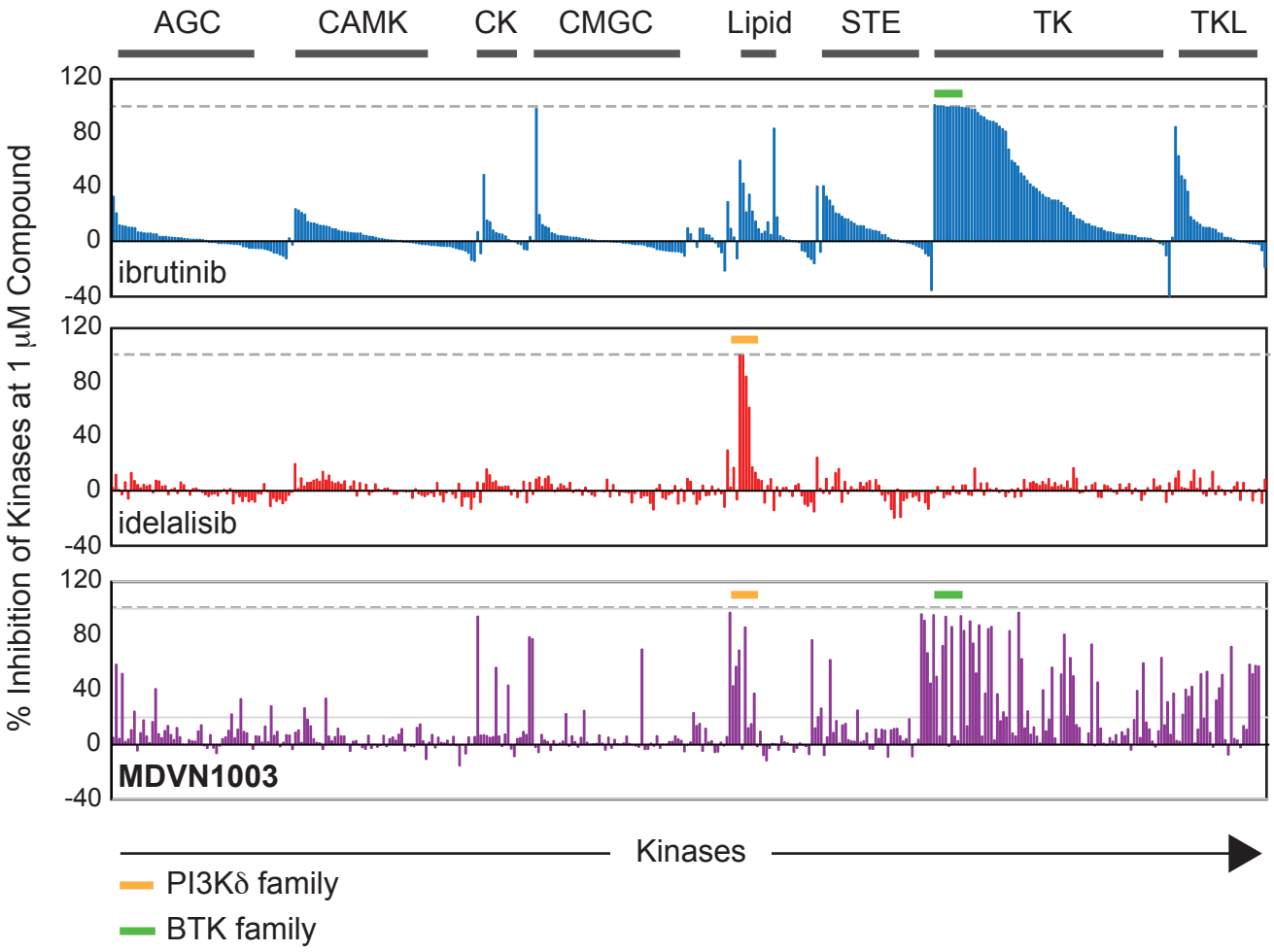

JPET Fast Forward. Published on March 15, 2017 as DOI: 10.1124/jpet.116.238022
This article has not been copyedited and formatted. The final version may differ from this version.

Figure 4

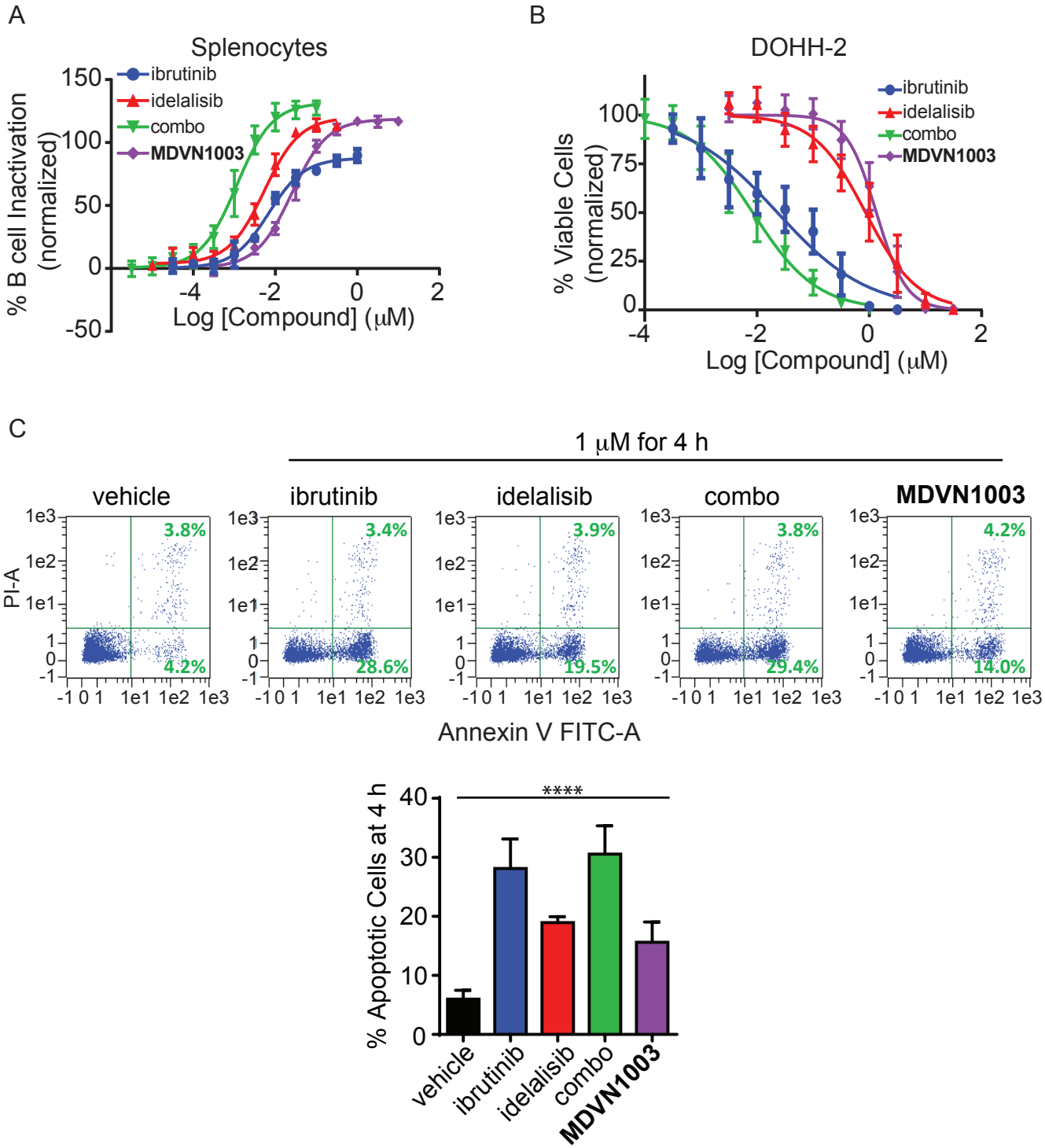

JPET Fast Forward. Published on March 15, 2017 as DOI: 10.1124/jpet.116.238022
This article has not been copyedited and formatted. The final version may differ from this version.

Figure 5

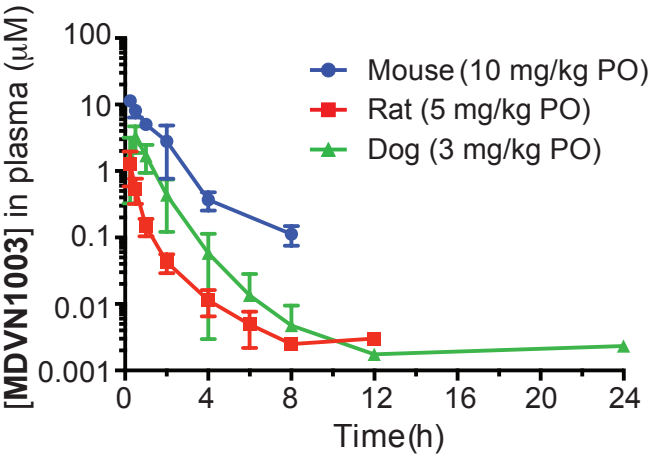

JPET Fast Forward. Published on March 15, 2017 as DOI: 10.1124/jpet.116.238022
This article has not been copyedited and formatted. The final version may differ from this version.

Figure 6